ARTICLE   OPEN

Check for updates

Monozygotic twins discordant for schizophrenia differ in maturation and synaptic transmission

Shani Stern [1,15✉], Lei Zhang[2,15], Meiyan Wang[2,15], Rebecca Wright[2], Idan Rosh[1], Yara Hussein [1], Tchelet Stern[1], Ashwani Choudhary[1], Utkarsh Tripathi [1], Patrick Reed[2], Hagit Sadis[1], Ritu Nayak[1], Aviram Shemen[1], Karishma Agarwal[1], Diogo Cordeiro[1], David Peles[1], Yuqing Hang[3], Ana P. D. Mendes[2], Tithi D. Baul[4], Julien G. Roth [5], Shashank Coorapati[2], Marco P. Boks [6], W. Richard McCombie[7], Hilleke Hulshoff Pol [6,8], Kristen J. Brennand [9,10], János M. Réthelyi[11], René S. Kahn [12,13], Maria C. Marchetto[14] and Fred H. Gage [2✉]

Schizophrenia affects approximately 1% of the world population. Genetics, epigenetics, and environmental factors are known to play a role in this psychiatric disorder. While there is a high concordance in monozygotic twins, about half of twin pairs are discordant for schizophrenia. To address the question of how and when concordance in monozygotic twins occur, we have obtained fibroblasts from two pairs of schizophrenia discordant twins (one sibling with schizophrenia while the second one is unaffected by schizophrenia) and three pairs of healthy twins (both of the siblings are healthy). We have prepared iPSC models for these 3 groups of patients with schizophrenia, unaffected co-twins, and the healthy twins. When the study started the co-twins were considered healthy and unaffected but both the co-twins were later diagnosed with a depressive disorder. The reprogrammed iPSCs were differentiated into hippocampal neurons to measure the neurophysiological abnormalities in the patients. We found that the neurons derived from the schizophrenia patients were less arborized, were hypoexcitable with immature spike features, and exhibited a significant reduction in synaptic activity with dysregulation in synapse-related genes. Interestingly, the neurons derived from the co-twin siblings who did not have schizophrenia formed another distinct group that was different from the neurons in the group of the affected twin siblings but also different from the neurons in the group of the control twins. Importantly, their synaptic activity was not affected. Our measurements that were obtained from schizophrenia patients and their monozygotic twin and compared also to control healthy twins point to hippocampal synaptic deficits as a central mechanism in schizophrenia.

Molecular Psychiatry; https://doi.org/10.1038/s41380-024-02561-1

INTRODUCTION

The prevalence of schizophrenia is approximately 1% worldwide [1], and full recovery of these patients is limited and the prognosis is guarded [2, 3]. Schizophrenia is defined in the *Diagnostic and Statistical Manual of Mental Disorders, Fifth Edition*, (*DSM-5*) by at least 2 of the following symptoms: delusions, hallucinations, disorganized speech, negative symptoms, and disorganized or catatonic behavior. At least one of the symptoms must be the presence of disorganized speech, delusions, or hallucinations. These signs and symptoms of the disturbance must persist for at least 6 months; during this time, the patient must experience at least one month of active symptoms and social or occupational deterioration problems over a significant period. These problems

are unique and not related to other conditions, e.g. psychoactive substances or neurologic conditions.

Although many studies have been conducted to elucidate the genes and molecules related to schizophrenia, it remains unclear as to which of the candidate genes are most critical to the disease. Post-mortem studies and neuroimaging technologies have shown differences between the brains of schizophrenia patients compared to healthy individuals. A decrease in brain volume in the medial-temporal areas, changes in the hippocampus and larger ventricles, and white matter tracts, and structural brain abnormalities are some of these alterations [4–6].

Neurotransmitter abnormalities have also been elucidated, especially in the dopaminergic system, although some studies

[1]Sagol Department of Neurobiology, Faculty of Natural Sciences, University of Haifa, Haifa, Israel. [2]Laboratory of Genetics, The Salk Institute for Biological Studies, La Jolla, CA, USA. [3]Razavi Newman Integrative Genomics and Bioinformatics Core, Salk Institute for Biological Studies, La Jolla, CA, USA. [4]Department of Psychiatry at the Boston Medical Center, Boston, MA, USA. [5]Institute for Stem Cell Biology & Regenerative Medicine, Stanford University School of Medicine, Stanford, CA, USA. [6]Department of Psychiatry, University Medical Center Utrecht Brain Center, Utrecht University, Heidelberglaan 100, 3584CX Utrecht, The Netherlands. [7]Cold Spring Harbor Laboratory, Cold Spring Harbor, New York, NY, USA. [8]Department of Experimental Psychology, Utrecht University, Heidelberglaan 1, 3584CS Utrecht, The Netherlands. [9]Nash Family Department of Neuroscience, Friedman Brain Institute, Pamela Sklar Division of Psychiatric Genomics, Black Family Stem Cell Institute, Icahn School of Medicine at Mount Sinai, New York, NY 10029, USA. [10]Department of Psychiatry, Department of Genetics, Yale Stem Cell Center, Yale University School of Medicine, New Haven, CT 06511, USA. [11]Molecular Psychiatry Research Group and Department of Psychiatry and Psychotherapy, Semmelweis University, Budapest, Hungary. [12]Department of Psychiatry, Icahn School of Medicine at Mount Sinai, New York, NY, USA. [13]Mental Illness Research, Education and Clinical Center, James J Peters VA Medical Center, New York, NY, USA. [14]Department of Anthropology, University of California San Diego, 9500 Gilman Drive, La Jolla, CA 92093, USA. [15]These authors contributed equally: Shani Stern, Lei Zhang, Meiyan Wang. ✉email: sstern@univ.haifa.ac.il; gage@salk.edu

2

also implicate other neurotransmitter systems such as gamma-aminobutyric acid (GABA), norepinephrine, serotonin, and NMDA glutamate receptors [7–10]. In addition to a genetic contribution, the environment also plays a key role in disease etiology [11]. This disorder is hereditary and the concordance of schizophrenia in monozygotic twins ranges from 41 to 79% [12–14]. Genome-wide association studies (GWAS) have been performed in schizophrenia with an approach to better understand the etiology of the disease. Many genes have been associated with schizophrenia [15–20]. Some of the associated genes include CACNA1C, DGCR8, DRD2, MIR137, NOS1AP, and NRXN1. More than 100 schizophrenia-related loci have been reported, although the GWAS loci identified failed to identify the high-risk genes (HRGs) related to schizophrenia [17, 21]. Single-nucleotide polymorphisms (SNPs) and their link with associated genes are often difficult to interpret, especially when the SNPs are in noncoding regions. Many methods have been attempted to identify risk genes linked to schizophrenia regulated by GWAS loci. For instance, integrating position weight matrix (PWM) and functional genomics [22, 23] or topologically associated domains that are generated by chromatin interaction experiments [24]. Using large databases of GWAS, transcriptome-wide associated studies (TWAS), large web-based platforms, multi- omics data, and gene expression in statistical models were used to predict HRGs in schizophrenia in an attempt to explain the high heritability of schizophrenia and provide mechanistic insights of the disease. Expression patterns of genes in schizophrenia neurons may further elucidate the molecular mechanisms of the disease and drug discovery [25]. The Psychiatry Genome Consortium wave 3 (PGC3) meta-analysis has reported 287 genomic loci containing common alleles associated with schizophrenia, highlighting the complex genetic architecture enriched by neurodevelopmental genes as well as synapse-related pathways as being of central importance [26].

For the past two and a half decades, human stem cell technology has been used to generate virtually any human cell type [27], and induced pluripotent stem cell (iPSC)-based models have advanced the study of neuropsychiatry disorders such as schizophrenia, depression, autism spectrum disorder, epilepsy, bipolar disorder, and Alzheimer's and Parkinson's diseases among others brain disorders and diseases [18, 28–34]. The first few studies demonstrating the generation of iPSCs from patients with schizophrenia were published a decade ago [28, 35, 36]. Some of the schizophrenia cases in these studies were described as idiopathic and others had demonstrated familial inheritance. There were no intrinsic deficits in iPSC pluripotency or self-renewal when derived from schizophrenia patients compared to controls that were reported [28, 34–36].

Chiang et al. [35] were the first to publish the generation of human iPSCs from schizophrenia patients with a mutation in the DISC1 gene that is known to be linked to schizophrenia [37]. They were the first to produce integration-free iPSC lines from schizophrenia patients showing the expression of the pluripotency markers, normal karyotypes, demethylation of CpGs in promoter regions of pluripotent genes, and the iPSC differentiation into the three germ layers. Neuronal changes have been reported also by Brennand et al. [28], who observed differences in iPSCs patient-derived neurons such as neuronal connectivity, decreased neurite number, and postsynaptic density protein 95 (PSD95) levels that were also reduced.

Gene expression profiles were also different in schizophrenia neurons with alterations in genes associated with cAMP, WNT pathways, and glutamate receptor expression. A few years later, the same lab reported that neurons that were derived from schizophrenia patients were hypoexcitable [34]. Pedrosa et al. [36] also demonstrated the potential use of iPSCs in modeling schizophrenia, showing that derived neurons expressed chromatin remodeling proteins, transcriptional factors, and synaptic proteins that were relevant to schizophrenia. A significant delay in the reduction of endogenous

OCT4 and NANOG expression was shown during differentiation in the schizophrenia lines. Na$^+$ channel function and GABA-ergic neurotransmission have recently been shown to be altered in neurons derived from iPSCs of schizophrenia patients [38]. These new approaches to neuropsychiatry disorders have the potential to address the problem of brain inaccessibility by providing the investigators with specific neurons of patients with proper diagnostic validity (or simply proper diagnoses). These studies have profoundly advanced our understanding of the disorder. However, due to the genetic heterogeneity of this disorder, a study where the patients have the same genetic background as the controls would have significantly helped to elucidate the mechanisms that are specific to schizophrenia since the variation between individuals may mask some of the phenotypes. An in-depth characterization of the neurophysiology and the transcriptome of patients' neurons compared to neurons from the same genetic background would help eliminate the noise and isolate the mechanisms of the disease.

In this study, iPSCs from monozygotic twins discordant for schizophrenia and a control group of healthy twins were differentiated into neural progenitor cells (NPCs), 2 months, and 4 months in vitro neurons. The advantage of this system is the similar genetic background of the affected and unaffected siblings (with depressive disorder), which minimizes the genetic diversity and allows us to focus on phenotypes that are specific to schizophrenia. The differentiated neurons were analyzed over a period from four weeks to two months, and the transcriptome (RNAseq), morphology, histology, and also functional assays measured with electrophysiology and microelectrode array (MEA) were used to compare the affected patients and their unaffected twin siblings (depressive disorder) to the control group. We found an immature state of dentate gyrus (DG) granule neurons that were derived from the schizophrenia patients, with an intermediate state in the neurons that were derived from the unaffected siblings (depressive disorder). An immature DG was previously shown to manifest an immature molecular profile in schizophrenia subjects, as well as in various animal models [39]. Our results further support this phenotype in a human cellular model. The most pronounced phenotype was an impairment of the synaptic transmission in the schizophrenia patients measured both with electrophysiology and at the gene expression levels.

MATERIALS AND METHODS
Patient selection
The recruitment of the subjects and biopsies were carried out in Utrecht, Netherlands at the Department of Psychiatry, University Medical Center (UMC) Utrecht. Monozygotic twin pairs discordant for schizophrenia and control monozygotic twin pairs from the twin cohort [40] were asked to participate in the study. Diagnosis of schizophrenia was made according to the Diagnostic and Statistical Manual of Mental Disorders (DSM)-IV. Control twins were excluded if they ever met the criteria for a psychotic or manic disorder substance dependence, had a first-degree relative with schizophrenia, or if were diagnosed with a neurological disorder. All participants gave their written informed consent. The Medical Ethical Committee of the UMC Utrecht approved this study and the experiments were under the Declaration of Helsinki. The Institutional Review Board (IRB) approval was obtained by Salk Institute and the samples were de-identified. Altogether, fibroblast cells from 5 twin pairs have been successfully reprogrammed by the staff of the Salk Institute Stem Cell Core Laboratory (subject age: 32–50 years). Two pairs of subjects are discordant for schizophrenia (age at onset of schizophrenia: 22–35 years) and 3 are healthy control twins (Fig. 1).

iPSC reprogramming and neuron differentiation
iPSCs were derived from fibroblasts for control and schizophrenia patients using the Cyto-Tune Sendai reprogramming kit (Invitrogen) according to the manufacturer's instructions. iPSCs were characterized for a normal karyotype (Supplementary File 1) as well as for pluripotency markers as previously described [41] (Fig. 1). iPSC colonies were cultured on Matrigel-coated plates using mTeSR medium (StemCell Technologies). Embryoid bodies (EBs) were formed by mechanical dissociation of iPSC colonies
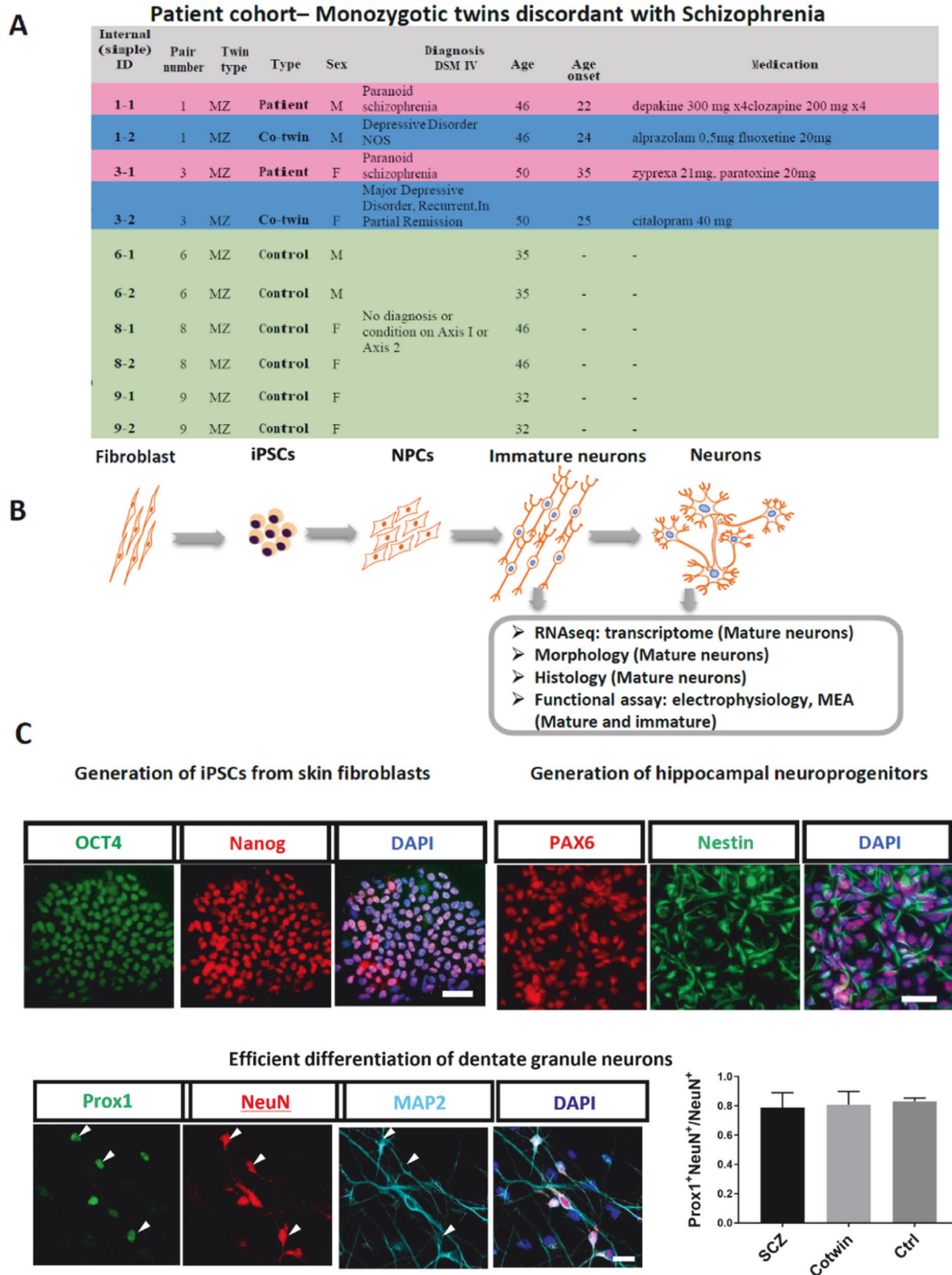
A Patient cohort– Monozygotic twins discordant with Schizophrenia

Internal (simple) ID	Pair number	Twin type	Type	Sex	Diagnosis DSM IV	Age	Age onset	Medication
1-1	1	MZ	Patient	M	Paranoid schizophrenia	46	22	depakine 300 mg x4clozapine 200 mg x4
1-2	1	MZ	Co-twin	M	Depressive Disorder NOS	46	24	alprazolam 0,5mg fluoxetine 20mg
3-1	3	MZ	Patient	F	Paranoid schizophrenia	50	35	zyprexa 21mg, paratoxine 20mg
3-2	3	MZ	Co-twin	F	Major Depressive Disorder, Recurrent,In Partial Remission	50	25	citalopram 40 mg
6-1	6	MZ	Control	M		35	-	-
6-2	6	MZ	Control	M		35	-	-
8-1	8	MZ	Control	F	No diagnosis or condition on Axis I or Axis 2	46	-	-
8-2	8	MZ	Control	F		46	-	-
9-1	9	MZ	Control	F		32	-	-
9-2	9	MZ	Control	F		32	-	-

B Fibroblast → iPSCs → NPCs → Immature neurons → Neurons

> RNAseq: transcriptome (Mature neurons)
> Morphology (Mature neurons)
> Histology (Mature neurons)
> Functional assay: electrophysiology, MEA (Mature and immature)

C

Generation of iPSCs from skin fibroblasts — OCT4 | Nanog | DAPI

Generation of hippocampal neuroprogenitors — PAX6 | Nestin | DAPI

Efficient differentiation of dentate granule neurons — Prox1 | NeuN | MAP2 | DAPI

Prox1⁺NeuN⁺/NeuN⁺ — SCZ, Cotwin, Ctrl

Fig. 1 Generation of neurons from healthy twin sets and from twin sets that are discordant for schizophrenia. A A table describing the cohort of patients and control individuals. The lines with the information of the affected patients are highlighted in pink and the unaffected twin siblings (depressive disorder) are highlighted in light blue. The green lines contain information about the healthy control twin sets. **B** A schematic of the reprogramming and differentiation and the experiments performed. **C** Upper row, left – Pluripotency markers were expressed in the reprogrammed iPSCs. Upper row, Right – Neural Progenitor cells (NPCs) expressed Nestin and PAX6–NPC-specific markers. Lower row – differentiated neurons expressed MAP2 and approximately 80% expressed Prox1, a marker that is specific for the DG granule neurons in neurons derived from the 3 groups of affected twin siblings, unaffected co-twin siblings, and healthy twin sets. Scale bars are 50 μm.

using dispase and then plated in ultra low-attachment plates. The mTeSR was replaced on the next day with DMEM/F12 (Invitrogen) supplemented with N2 and B27. For EB differentiation, floating EBs were treated with DKK1 (0.5 µg /ml), SB431542 (10 µM), noggin (0.5 µg/ml) and cyclopamine (1 µm) for 20 days. To obtain neural progenitor cells (NPCs), the embryoid bodies were plated onto poly-L-ornithine/laminin- coated plates. The rosettes were manually collected and dissociated with accutase after 1 week and plated onto poly-L-ornithine/laminin-coated plates in NPC media containing DMEM/F12, N2, B27, 1 µg/ml laminin, and 20 ng/ml FGF2. To obtain neurons, NPCs were differentiated in DMEM/F12 supplemented with N2, B27, 20 ng/ml BDNF (Peprotech), 1 mM dibutyrl-cyclicAMP (Sigma), 200 nM ascorbic acid (Sigma), 1 µg/ml laminin, and 620 ng/ml Wnt3a (R&D) for 3 weeks. Wnt3a was removed after 3 weeks. Neurons were infected with the Prox1::eGFP lentiviral vector [29] at 8 days of differentiation and the experiments were performed in the Prox1-positive neurons. The neuronal cultures were dissociated and replated on poly-L-ornithine/laminin coated coverslips at 2 weeks using accutase. All cells were regularly tested for mycoplasma.

Immunocytochemistry (ICC)
Cells on glass coverslips were fixed in 4% paraformaldehyde for 15 min. The cells were then blocked and permeabilized in PBS containing 0.1–0.2% Triton X-100 and 10% horse serum. Coverslips were then incubated with the primary antibody in the blocking solution overnight at 4 °C. The coverslips were washed in Tris-buffered saline and incubated with the secondary antibodies for 30 min at room temperature and counterstained with DAPI. The coverslips were then washed and mounted on slides using Fluoromount-G (Southern Biotech), and dried overnight in the dark. The antibodies used for pluripotency and neuronal characterization were anti-hOct4 (Cell Signaling, Danvers, MA, USA 2840 S), anti-hNanog antibody (Cell Signaling 4903 S), anti-MAP2 (Abcam 5392) anti-PAX6 (Abcam ab109233), anti-Nestin (Abcam ab105389), anti-NeuN (Abcam ab177487), and anti-PROX1(Millipore MAB5654).

Sholl analysis
Differentiated neurons were traced using Neurolucida (MBF Bioscience, Williston, VT). Only neurons that were PROX1-positive were included in this analysis. The morphology of the neurons was quantified using Neurolucida Explorer (MBF Bioscience, Williston, VT). Sholl analysis was performed using Neurolucida Explorer's sholl analysis option. This analysis specified a center point within the soma and created a grid of concentric rings around it with radii increasing in 10 µm increments. Neuronal complexity was determined by recording the number of intersections within each ring.

Electrophysiology
The coverslips with neuronal cultures were transferred to a recording chamber at 2 time points - 4 weeks and 2 months - with artificial cerebrospinal fluid (ACSF) containing (in mM): 10 HEPES, 4 KCl, 2 CaCl2,1 MgCl2, 139 NaCl, and 10 D-glucose (310 mOsm, pH 7.4). Whole-cell patch-clamp recordings were performed from Prox1-positive neurons. Patch electrodes were filled with an internal solution containing (in mM): 130 K-gluconate, 6 KCl, 4 NaCl, 10 Na-HEPES, 0.2 K-EGTA, 0.3 GTP, 2 MgATP, 0.2 cAMP, 10 D-glucose, 0.15% biocytin, and 0.06% rhodamine. The pH and osmolarity of the internal solution were adjusted to a pH of 7.4 and an osmolarity of 290 mOsm. The signals were amplified with a Multiclamp700B amplifier (Sunnyvale, CA, USA) and recorded with Clampex 10.3 software (Axon Instruments, Union City, CA, USA). Data were acquired at a sampling rate of 20 kHz and analyzed using Clampfit-10 and the software package MATLAB (release 2014b; The MathWorks, Natick, MA, USA). All measurements were conducted at room temperature.

Analysis electrophysiology
Total evoked action potentials. The cells were typically held in current-clamp mode at −60 mV and current injections were given starting 12 pA below the holding current, in 3 pA steps of 400 ms in duration. A total of 20 depolarization steps were injected. Neurons with a holding current of more than 50 pA were discarded from the analysis. The total number of action potentials was counted in 20 depolarization steps.

Action potential shape analysis. The first evoked action potential was used for this analysis (with the minimal injected current needed for an action potential to occur). The spike threshold was the membrane potential of the first maximum in the second derivative of the voltage by time. The fast afterhyperpolarization (AHP) amplitude was calculated as the difference between the threshold for an action potential and the membrane potential 5 ms after the membrane potential returned to cross the threshold value after the action potential resumed. The spike amplitude was calculated as the difference between the maximum membrane potential during an action potential and the threshold. The spike width was calculated as the time it took the membrane potential to reach half the spike amplitude in the rising part of the spike to the descending part of the spike (full-width at half-maximum).

The membrane resistance was calculated around the resting membrane potential by measuring the current at −70 mV and then at −50 mV. The membrane resistance was calculated by dividing 20 mV by the difference in these currents.

Sodium and potassium currents. The sodium and potassium currents were acquired in voltage-clamp mode. The cells were held at −60 mV, and voltage steps of 400 ms were then given in the range of −90 to 80 mV. The fast potassium current measurement was obtained as the maximal current within a few milliseconds after the depolarization step. The slow potassium currents were obtained at the end of the 400 ms depolarization step. The sodium current was obtained by subtracting the minimum current, representing the inward sodium current from the current after stabilizing from the transient sodium current.

Excitatory postsynaptic currents recordings. Excitatory postsynaptic currents (EPSCs) were measured by voltage clamping the cells at −60 mV after application of 40 µM of bicuculline, a GABA_A antagonist. The analysis was performed using semi-manual Matlab scripts.

Multiwell microelectrode array (MEA) recordings and analysis
To record the spontaneous activity of neurons derived from schizophrenia twins and healthy twins, neurons at 31-day differentiation were seeded in 96 wells MEA plates from Axion Biosystems (San Francisco, CA, USA). Each subject's cells were plated in replicates of 6 and seeded with 10,000 neurons in each well. Cells were fed every 2–3 days and electrical activity was recorded every 3–4 days from day 37 of neuronal differentiation using the maestro MEA system and Axis software (Axion Biosystems). Voltages were recorded at a frequency of 12.5 kHz and bandpass filtered between 10 Hz and 2.5 kHz. Spike detection was performed using an adaptive threshold set to 5.5 standard deviations above the mean activity of each electrode. Following 5 min of plate adaptation time, recordings were performed for 10 min. Multielectrode data analysis was performed using the Axion Biosystems Neural Metrics Tool, which calculated standard spike-related measurements. Bursts were detected with an adaptive Poisson algorithm for high spiking activity that occurred on a single electrode. Variables were averaged across subject replicates and plotted by groups for each day of the recordings. A two-way ANOVA was used to compare the electrical activity in the 3 groups.

FACS sorting
We have prepared the neurons for RNA-seq according to a published FACS protocol [42]. Briefly, five- week-old neurons were dissociated and CD184−/CD44−/CD15−/CD24+ cells (Miltenyi Biotec, cat. number 130-103-868, 130-113-334, 560828, 130-099-399, respectively) were collected and subjected to Stranded mRNA (PolyA +)-Seq Library Prep. A total of 1000 ng of RNA was used for library preparation using the Illumina TruSeq RNA Sample Preparation Kit. The libraries were sequenced on Illumina HiSeq2500 with 50 bp single-end reads.

RNA sequencing analysis
The raw fastq reads underwent sequence alignment using the Spliced Transcripts Alignment to a Reference (STAR) [43] and HOMER (http://homer.ucsd.edu/homer/ngs/rnaseq/index.html). Both raw count and transcripts per million (tpm) quantified matrix for all experiments were generated. Principal component analysis (PCA) and a heatmap were generated based on the whole tpm matrix in R 3.6.1 using gplots, and Differentially expressed genes (DEG) analysis was performed using DESeq2 [44]. Pooled schizophrenia patients, as well as non-affected co-twins, were compared with control twin samples. Also, schizophrenia patients were compared with their corresponding co-twin samples respectively. A heatmap of the DEGs were generated in R, and Functional Enrichment for the DEGs was performed on WebGestalt (http://www.webgestalt.org/).

Also, Venn diagrams were generated on the online Venn webtool (https://bioinformatics.psb.ugent.be/webtools/Venn/).

GWAS Genes and DEGs intersection
We used the GWAS Catalog (https://www.ebi.ac.uk/gwas/) and searched for the term "schizophrenia". We performed an intersection between GWAS genes and DEGs. The intersection genes were computed by comparing the symbols of GWAS genes and DEGs (after the symbol standardization). The intersected genes graph was generated by Matlab's wordcloud function, down-regulated genes were painted in blue, and up-regulated genes in red. The font size is proportional to the number of GWAS studies that included this gene with p-value < 0.01.

Statistical analysis
The default comparison analysis when not specified was the student t-test. For comparisons of a few groups, we used a one-way ANOVA and the function multcompare of Matlab to calculate the statistics between the different groups when using the one-way ANOVA. We have verified the Normal distribution of the data using the kstest of Matlab, which performs a Kolmogorov-Smirnov test. To perform the test, we have subtracted the mean of the samples and normalized them by the standard deviation of the samples, and then performed the kstest.

RESULTS
All patients, as well as control lines, differentiate with a high efficiency into hippocampal DG granule neurons
Fibroblasts were produced after a skin biopsy from a total of 2 pairs of monozygotic twins discordant for schizophrenia and 3 pairs of control (healthy) twins. The data were partitioned into 3 groups: the affected twin (2 patients), the unaffected twin sibling (2 unaffected co-twins; depressive disorder), and 6 control individuals from the healthy twins. Figure 1A presents the details about the patients, their unaffected co- twin (depressive disorder), and the control twins. Sendai reprogramming was performed on the fibroblasts and the patients, their co-twin, and the control twins and iPSCs were prepared. The iPSCs from all the lines exhibited pluripotency markers (Fig. 1C, left). We next prepared hippocampal NPCs [29] and, from these, we differentiated neurons and performed experiments on these neurons at 2 maturation time points (Fig. 1B for the schematics). All the lines from the 3 groups were differentiated between 3-5 times to validate the robustness of the results. Figure 1C, right, presents ICC performed on the NPCs for specific markers. All the lines expressed NPC-specific markers. Figure 1C (bottom row) presents the efficient generation of DG granule neurons with approximately 80% Prox1 positive neurons. To further validate that the neurons are indeed DG granule neurons, we have compared their transcriptome to human postmortem DG granule neurons [45] and found a significant enrichment of the genes expressed in our cells and the human postmortem DG (Supplementary Fig. 4).

DG neurons derived from schizophrenia patients are less arborized and exhibit delayed maturation, while neurons derived from the co-twin exhibit a mid-state between the other 2 groups
We next performed imaging of the DG neurons derived from the 3 groups (affected twins, unaffected co- twins; depressive disorder, and controls) of rhodamine-filled neurons at 8 weeks post-differentiation. The neurons were filled with rhodamine during patch-clamp recordings. We used a one-way ANOVA for the comparisons in Fig. 2 Sholl analysis and capacitance measurements reveal that the neurons derived from the schizophrenia-affected twin siblings were the least arborized of all the 3 groups. Figure 2A presents example traces of rhodamine-filled neurons. Figure 2B presents the average sholl analysis of $n = 16$ control neurons, $n = 26$ co-twin neurons, and $n = 29$ affected neurons. Figure 2C presents the number of branches in each of the groups which were significantly smaller in the schizophrenia neurons

compared to the neurons derived from the controlsc. Figure 2D presents the maximal branch length, which was not significantly different between the groups. The soma size was smaller in the neurons derived from the schizophrenia patients compared both to their co-twins and the controls (Supplementary Fig. 8A). Additionally, the total dendritic tree was smaller in the neurons derived from the schizophrenia patients compared to the controls, and also the total dendritic tree of neurons derived from the co-twins was smaller compared to the controls (Supplementary Fig. 8B). We have also analyzed the capacitance of the membrane of the neurons that were measured during the electrophysiology experiments from the 3 groups when the neurons were at 8 weeks after the start of the differentiation. The neurons derived from the schizophrenia patients had the smallest average capacitance, whereas the neurons derived from the unaffected co-twin (depressive disorder) had an average capacitance that was in between the affected twin and the control average capacitances (Fig. 2E, F). Since the membrane capacitance is proportional to the surface area of the neuron, this measurement further supported the finding that the neurons derived from the schizophrenia patients were smaller and less arborized, and the neurons derived from the unaffected co-twin (depressive disorder) were in between the other two groups.

The membrane input conductance also signifies the maturity of the neurons and is directly affected by ion channels such as the inward rectifying potassium channels and other ion channels that are open at the resting membrane potential. Measurements of the membrane conductance also revealed that the 3 groups (affected, unaffected co-twin, and control) were different from one another (Fig. 2G, H). The affected twin neurons had the highest input conductance (0.56 ± 0.07 nS), whereas the unaffected co-twin group (depressive disorder) had an average input conductance that was in between the affected neurons and the control neurons (0.46 ± 0.06 nS). The control neurons had the lowest average membrane conductance (0.24 ± 0.01 nS). The high membrane conductnace of the neurons derived from the schizophrenia patients means that they had the most number of ion channels that were open at the resting membrane potential such as the inward rectifying ion channels and Hyperpolarization-activated cyclic nucleotide-gated (HCN) channels. This finding further supports the observation that such neurons were delayed in their maturation or have deficits in their ion channels. The resting membrane potential is another measure of neuronal maturation and is also related to the number of ion channels on the membrane. In this measure, too, we found that the groups were different from one another (Fig. 2I, J). The affected twin group had the most depolarized resting membrane potential (-40.6 ± 1.8 mV), whereas the unaffected twin group (depressive disorder) was again in the middle among the other 2 groups (-46.3 ± 1.7 mV), and the control twins had the least depolarized membrane potential (-52.8 ± 0.8 mV), indicating the control group displays the most mature state.

Transcriptional changes in DG neurons derived from the schizophrenia patients compared to their unaffected co-twin (depressive disorder) and compared to the control twins
To further understand the mechanisms involved in DG neuronal changes in schizophrenia, we next performed RNA sequencing on RNA that was extracted from sorted DG granule neurons (see methods). The neurons were dissociated and RNA was prepared at approximately 5-6 weeks post-differentiation. Neurons derived from 2 iPSC clones were sent for sequencing for each of the subjects and there was a significant difference in expression of a few hundreds of genes after correction for multiple hypotheses (see Methods) between the groups. For the first analysis, neurons derived from the affected twins (the affected and unaffected co-twins) were pooled together and compared to neurons derived from the healthy twin pairs. Figure 3A presents a PCA on the left.

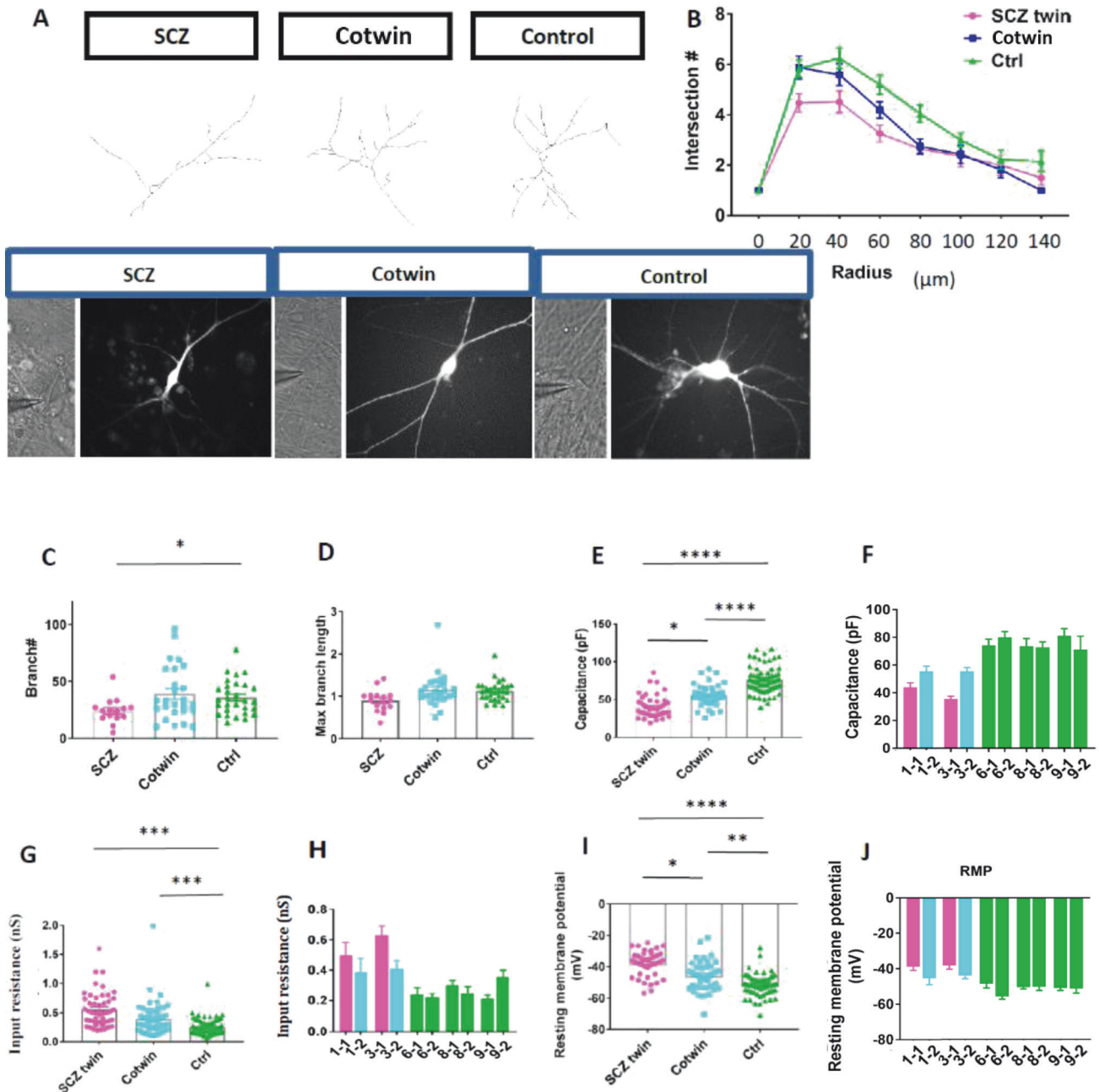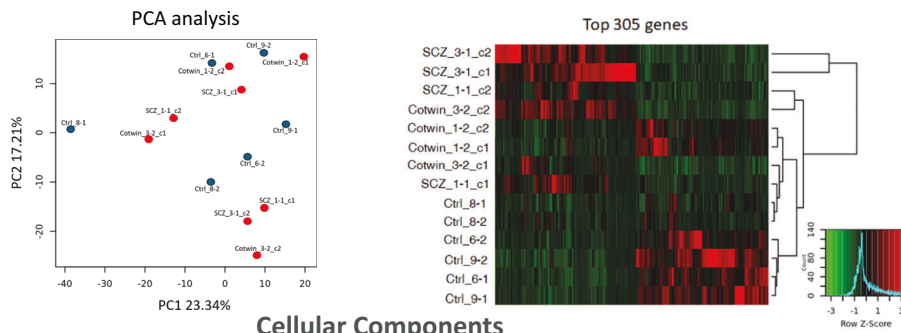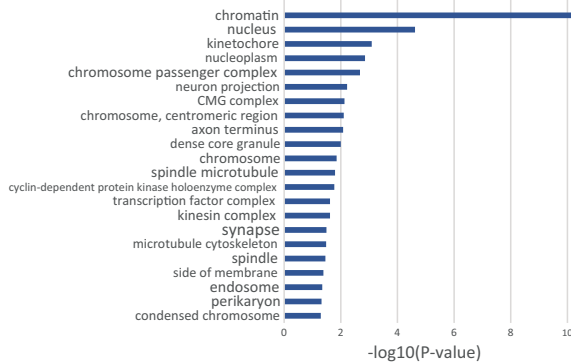## Sholl analysis showed a less complex morphology in SCZ neurons

Fig. 2 Immature features of neurons derived from the schizophrenia patients and an intermediate state of the neurons derived from the unaffected co-twin siblings (depressive disorder). A Example traces of a schizophrenia, co-twin, and a control neuron. **B** Sholl analysis shows that neurons derived from the schizophrenia patients are less arborized than the neurons derived from their unaffected twin siblings, but both groups are less arborized than neurons derived from the healthy twin sets. **C** The number of branches was slightly reduced in the schizophrenia neurons compared to the neurons derived from their co-twin, and significantly reduced when compared to control neurons. **D** The maximum number of branches was reduced, but not significantly, in the schizophrenia neurons compared to the neurons derived from the co-twins and controls. **E, F** The neurons derived from the affected twin siblings had the smallest capacitance. The neurons derived from the unaffected twin siblings had a higher capacitance than the affected twin siblings, but smaller than the healthy control twins. **G H** The neurons derived from the affected twin siblings had the highest membrane resistance. The neurons derived from the unaffected co-twin siblings had a smaller membrane resistance than the affected twin siblings but larger than the healthy control twins. **I, J** The neurons derived from the affected twin siblings had the most depolarized resting membrane potential. The neurons derived from the unaffected co-twin siblings had a resting membrane potential that was less depolarized than the affected twin siblings but more depolarized compared to the healthy control twins. The data acquired in this figure was obtained from one clone of each of the iPSC lines and 3-4 differentiation cycles for each of the lines. *represents $p < 0.05$, **represents $p < 0.01$, *** represents $p < 0.001$, **** represents $p < 0.0001$.
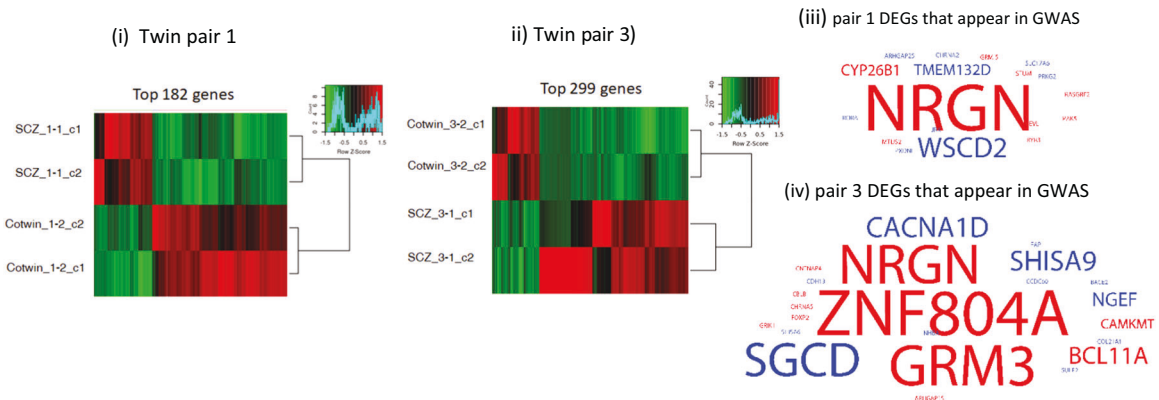
A Alterations in transcriptome in neurons derived from MZ twins discordant for SCZ

Pooled SCZ (affected + non affected) twins VS Neurotypical twins

PCA analysis

Top 305 genes

B

Cellular Components

C Transcriptome alteration in neurons derived from SCZ compared to the twin sibling

(i) Twin pair 1

ii) Twin pair 3)

(iii) pair 1 DEGs that appear in GWAS

(iv) pair 3 DEGs that appear in GWAS

D Gene overlap analysis

On the right, a heatmap of the top 305 differentially expressed genes is presented, showing gene expression changes between the affected twin pairs and the control twin pairs. Genes involved in dentate gyrus development (e.g., *LEF1*, *CALB1*) were identified. Performing Gene Ontology (GO) cellular component analysis, we found a few dysregulated pathways that are presented in Fig. 3B. These include synapse, neuron projection, and axon terminus. These transcriptional changes give further support to our morphological and electrophysiological findings. Genes in the canonical wnt pathway were also dysregulated (e.g., *LEF1*, *GLI3*,

Fig. 3 Transcriptomic analysis between the affected twin set and the control twin sets reveals synapse, neuron projection, and axon terminus dysregulated pathways. A A total of 305 differentially expressed genes were found between the affected twin sets (both twins) and the healthy twins. A PCA plot of the gene expression data shown on the left. On the right, a heatmap of the 305 differentially expressed genes is presented. **B** Significantly dysregulated pathways between the neurons derived from the affected twin sets (both the siblings) compared to the neurons derived from the healthy twin sets are presented. **C** (i-ii) Heatmaps of the differentially expressed genes in the two affected twin sets (a comparison between the affected and unaffected twin) (iii-iv) Genes that appear as DEGs in our dataset as well as in GWAS. Down-regulated genes are presented in blue, and up-regulated genes in red. The font size is proportional to the number of GWAS studies that included this gene with p-value < 0.01. **D** Three different comparisons were performed. The affected twins (both siblings) compared to the healthy twins, the affected twin vs. their unaffected co-twin sibling (depressive disorder) in twin set 1, and similarly in twin set 3. Venn diagram reveals unique and shared genes between three comparisons. The data acquired in this figure was obtained from two biological replicates (different iPSC clones) for each of the lines.

SIX3), providing more evidence linking this pathway to neuropsychiatric disorders [46–49]. When we compared the twin affected by schizophrenia to the unaffected co-twin (depressive disorder) (2 comparisons), we also found a few hundred differentially expressed genes. Figure 3C (i-ii) presents the heatmaps of the DEGs in the 2 discordant twin pairs. Figure 3C (iii-iv) show common genes that are differentially expressed in our dataset and appear in published GWAS. Down-regulated genes are shown in blue, and up-regulated genes in red. The most pronounced gene that is dysregulated in both pair of twins and also comes up as associated in several GWAS is the NRGN gene. Interestingly, this gene encodes a postsynaptic protein kinase substrate that binds to calmodulin in the absence of calcium. This gene was reported also as a key associated gene for both schizophrenia and Autism Spectrum Disorder [19, 20]. Figure 3D presents the shared DEGs between control and schizophrenia-affected patients. The 3 different comparisons (2 affected twin pairs vs. healthy twin pairs, and the 2 comparisons of the affected vs. unaffected twins discordant for schizophrenia) showed few shared genes.

Reduced rate of excitatory postsynaptic currents in neurons derived from the affected twins

We voltage-clamped the neurons at −60 mV to measure spontaneous excitatory postsynaptic currents (sEPSCs) after the application of bicuculine to block inhibitory postsynaptic currents. We have previously shown that 10-15% of the neurons are GABAergic neurons [29, 41]. The neurons derived from the patients with schizophrenia had a drastic reduction in the EPSC frequency when compared to their unaffected co-twins (depressive disorder) or the healthy twin pairs (Fig. 4A left for representative traces and Fig. 4A right for averages over 23 neurons derived from the schizophrenia patients, 20 neurons derived from the unaffected co-twin (with depressive disorder), and 32 neurons derived from the healthy twins). The average amplitude of EPSCs was not changed between neurons derived from the 3 groups of control, unaffected co-twins (depressive disorder), and affected twins with schizophrenia (Fig. 4A right). The data indicate a pre-synaptic deficit in schizophrenia neurons, which is consistent with previous reports [35]. Additionally, when blocking AMPA-mediated synaptic transmission by the application of 10 μM CNQX, we have measured a reduction of the percentage of neurons that exhibit NMDA-mediated excitatory postsynaptic currents in those derived from both the schizophrenia patients and their co-twins compared to neurons derived from healthy individuals (Supplementary Fig. 3).

Going back to the transcriptomics analysis, we next plotted the top 20 DEGs between the neurons derived from the affected twins (both affected and unaffected twin siblings (depressive disorder)) compared to neurons derived from the control twins (Fig. 4B, left). Of these 20 genes, 6 were synapse-related (marked in purple). The HTR7 gene, a serotonin receptor, marked in red, is associated with schizophrenia [50, 51]. We also performed GO analysis on the comparisons between neurons derived from each affected twin and his unaffected co-twin (depressive disorder). The dysregulated pathways were highly shared when comparing the affected and
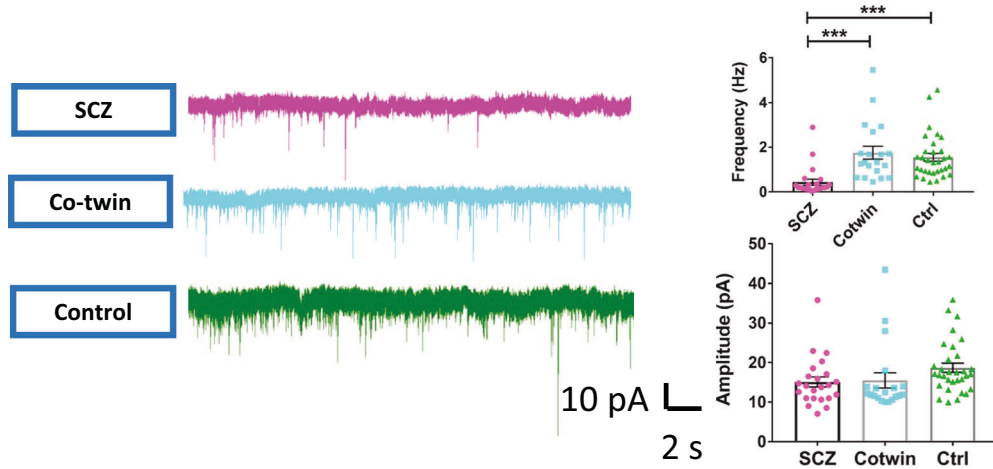
unaffected twin sets. For pair number 1, the dysregulated pathways included "Synapse" ($p = 0.000083$, FDR = 0.002), "Cell junction" ($p = 0.00014$, FDR = 0.002), and "Postsynaptic cell membrane" ($p = 0.00017$, FDR = 0.002). In pair 3, the most dysregulated functional annotations were similarly "Cell junction" ($p = 0.0072$, FDR = 0.17), "Postsynaptic cell membrane" ($p = 0.0096$, FDR = 0.17), and "Synapse" ($p = 0.021$, FDR = 0.25). Overall, our results demonstrate how a synaptic impairment is highly involved in schizophrenia. The changes that we see in the electrophysiology relate more to the pre-synapse, but compensation mechanisms may relay these changes to the post-synapse [52].

We additionally analyzed the pooled siblings with schizophrenia and compared them to the pooled controls, the siblings with schizophrenia and compared them to the pooled co-twins, and the pooled co- twins and compared them to the pooled controls (Supplementary Fig. 1). Interestingly, when pooling the affected siblings together and comparing them to their unaffected twins, there was only one enriched KEGG pathway (neuroactive ligand receptor interaction). Only 4 genes were significant when pooling the affected twins vs. the pooled co-twins, and these are presented in Supplementary File 2 and include the genes CALB1 (a calcium binding protein) and KCNIP4 (a potassium voltage gated channel). This emphasizes that although the pathways are shared when comparing each of the affected sibling with his co-twin, the genes that play a role are different in the two twin pairs. To elucidate whether the pre-synaptic deficit is related to the neuronal activity, we next performed recordings using a multi-electrode array (MEA) (Fig. 4C). The neurons derived from the affected twins with schizophrenia had a reduced number of spikes, a reduced number of bursts, and a reduced number of network bursts throughout the differentiation period (see Supplementary Files 6–8 for the statistical analysis using a 2-way ANOVA for the number of spikes, the number of bursts, and the number of network bursts accordingly). Interestingly, the neurons derived from the unaffected co-twin (depressive disorder) exhibited an increase in the number of spikes and the number of bursts. This increased excitability may act as a protective mechanism for a less connected neuronal network that exhibits more spontaneous activity and compensates for the reduced connections.
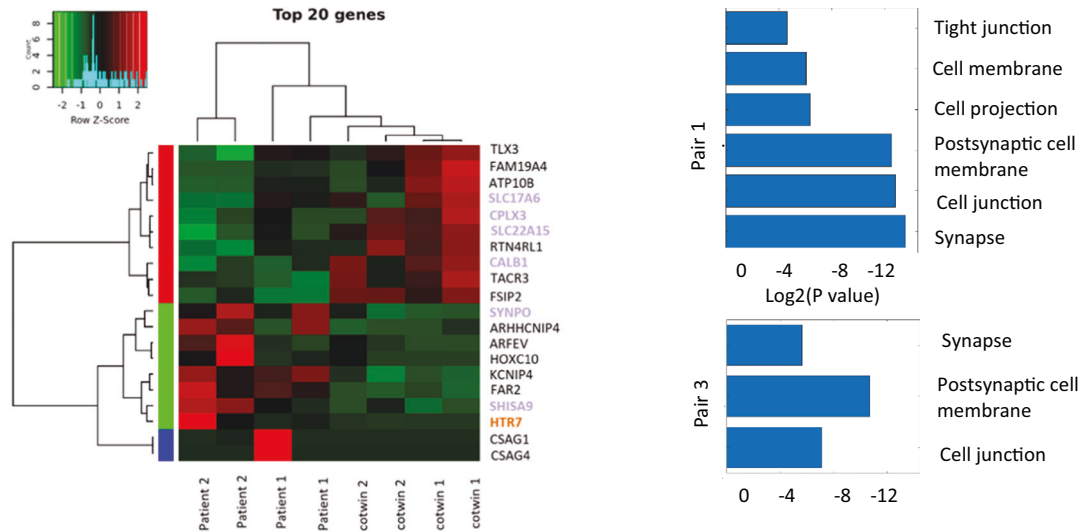
Intrinsic hypoexcitability of schizophrenia patient-derived neurons

To explore whether the reduced neural activity of schizophrenia neurons is rooted in an intrinsic deficit, we next measured the number of action potentials that were evoked in 20 voltage depolarization steps (see Methods section). The number of action potentials that were evoked in the affected twins was significantly reduced compared to the controls and the unaffected co-twins (depressive disorder). Additionally, the neurons derived from the unaffected twins were in an intermediate state and they too were significantly hypoexcitable compared to the control neurons (Fig. 5A left for representative traces and Fig. 5A right for averages over 38 control neurons, 30 neurons derived from the unaffected
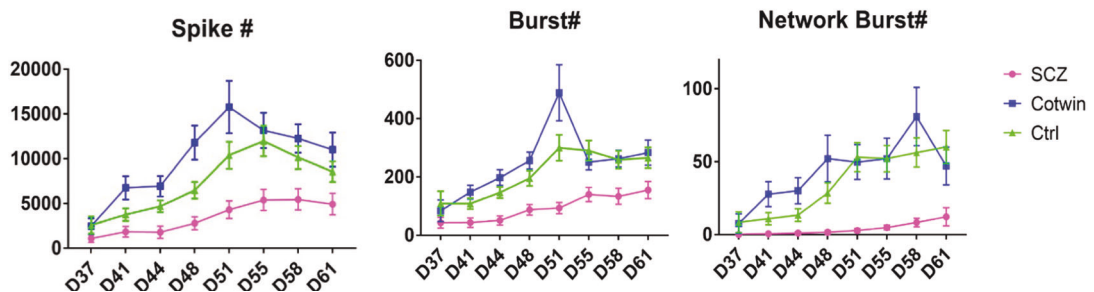
A Reduced EPSC frequency in SCZ neurons indicates deficits inpresynaptic neurotransmission

B Synapse related genes are dysregulated

C Multielectrode array (MEA) analysis revealed reduced neuronal activity in SCZ neurons

co-twins (depressive disorder), and 35 derived from the affected twins). Analysis of the spike shape also revealed 3 different groups with distinct states: the neurons derived from the healthy controls, the neurons derived from the unaffected co-twins (depressive disorder) that were in an intermediate state between the affected twin and the healthy controls, and the neurons derived from the affected twin siblings. Figure 5B shows that the width of the action potential was wider in the neurons derived from the affected twins and also wider, but to a smaller extent, in the unaffected co-twin (depressive disorder) when compared to the control neurons.

Fig. 4 Synaptic deficiency in the affected twin siblings. A A reduction in the rate of synaptic events measured in patch-clamp experiments was observed in the affected twin sibling but not in the unaffected co-twin sibling (depressive disorder). On the left are representative traces and, on the right, the averages are presented. The amplitude of the synaptic events was not affected, implying that the changes are mostly related to the pre-synapse. **B** On the left are the top 20 dysregulated genes when pooling the affected twins (both siblings) and comparing them to the healthy twins. Many genes that are synapse-related are in the top 20 genes (these genes are marked in purple). In red is a gene that has been associated with schizophrenia before [50, 51]. On the right are the dysregulated pathways when comparing the neurons derived from the affected twin sibling to the unaffected twin sibling for both pairs of discordant twins. The top 3 dysregulated pathways in both pairs are "Synapse"," Postsynaptic cell membrane", and "Cell junction," despite there being few shared dysregulated genes between the 2 pairs of discordant twins. **C** Multi- electrode array experiments show that the number of spikes and the number of bursts are reduced in the neurons derived from the schizophrenia patients but increased in the unaffected co-twin siblings. This may contribute to the mechanisms by which these siblings are not affected by schizophrenia. The data acquired in this figure was obtained from 3-4 differentiation cycles for each of the lines. ***represents $p < 0.001$.

◄

The spike amplitude was smaller in the neurons derived from the affected twin compared to the other 2 groups. The threshold for evoking an action potential was unaffected. And finally, the amplitude of the fast AHP was smaller in neurons derived from both the affected and unaffected twins (depressive disorder) compared to the neurons derived from the healthy control neurons.

Three distinct groups were observed throughout the maturation of the DG neurons

We next asked whether the maturation delay was exhibited in earlier time points. We analyzed the recordings at an earlier time point of 4 weeks' post-differentiation. The neurons were immature at this stage and most of them still did not have much evoked or spontaneous activity. However, measuring some neurophysiological properties we could see that the 3 groups had three different rates of maturation. At 4 weeks, the neurons derived from the affected twins had a smaller capacitance than the other 2 groups (Fig. 6A, $p = 4.6e-7$ compared to neurons derived from the unaffected co-twins, $p = 3.8e-13$ compared to neurons derived from the healthy twins, and p = 0.19 between neurons derived from the control and the unaffected twins), but at 2 months 3 distinct groups were significantly different from each other (Fig. 6A, $p = 0.0029$ for neurons derived from the schizophrenia patients compared to the unaffected co-twins, $p = 8e-15$ for neurons derived from the affected twins compared to the healthy twins, and $p = 1.3e-9$ for neurons derived from the unaffected co-twin compared to the healthy twins). The input conductnace at 4 weeks was significantly and extensively larger in the neurons derived from the affected twins (Fig. 6B, $p = 4.5e-5$ for neurons derived from the schizophrenia patients compared to the unaffected co-twins, $p = 2.1e-10$ for neurons derived from the affected twins to the healthy twins, and $p = 0.04$ for neurons derived from the unaffected co-twin compared to the healthy twins), but at 2 months the neurons derived from the affected and non-affected co-twins were significantly larger than the neurons derived from the controls (Fig. 6B, $p = 0.26$ for neurons derived from the schizophrenia patients compared to the unaffected co-twins, $p = 3.7e- 9$ for neurons derived from the affected twins compared to the healthy twins, and $p = 2.8e-5$ for neurons derived from the unaffected co-twins compared to the healthy twins). Also, notably, the input resistance drops for the schizophrenia twins by more than two-fold. This, together with the other data in this figure, suggests that early on the changes are even stronger and that schizophrenia is in fact a neurodevelopmental disorder although the onset is mainly during early adulthood.

The resting membrane potential was much more depolarized in the neurons derived from the affected twins at 4 weeks (Fig. 6C $p = 1.7e-4$ for neurons derived from the schizophrenia patients compared to the unaffected co-twins, $p = 6.1e-5$ for neurons derived from the affected co-twins to the healthy twins, and $p = 0.62$ for neurons derived from the unaffected co-twins compared to the healthy twins), and at 2 months the 3 groups were significantly different from each other, with the neurons

derived from the affected twins having the most depolarized threshold, then the neurons derived from the unaffected twins, and finally the most hyperpolarized resting membrane potential belonging to the neurons derived from the healthy controls (Fig. 6C $p = 0.025$ for neurons derived from the schizophrenia patients compared to the unaffected twins, $p = 4.5e-10$ for neurons derived from the affected twins to the healthy twins, and $p = 1.6e-4$ for neurons derived from the unaffected co-twins compared to the healthy twins).

Both the sodium and the potassium currents started as smaller currents in the neurons derived from the schizophrenia twins, with the unaffected co-twin in an intermediate state between the affected twins and the control (for sodium at −20 mV, $p = 4.7e-6$ control-schizophrenia patients, $p = 0.024$ co-twin- schizophrenia patients, $p = 0.045$ control-controls, for potassium at 20 mV, $p = 5.5e-6$ control-schizophrenia, $p = 0.056$ co-twin-schizophrenia, $p = 0.039$ co-twin-control). At 2 months, the neurons derived from the schizophrenia patients still had reduced sodium currents (Fig. 6D–I, For sodium at −20 mV, $p = 0.0053$ control-schizophrenia, $p = 0.24$ co-twin-schizophrenia, $p = 0.158$ co-twin-control, For potassium at 20 mV, $p = 0.0034$ control-schizophrenia, $p = 0.5$ co-twin-schizophrenia, $p = 0.005$ co-twin-control). Representative traces of the sodium and potassium currents are presented in Fig. 6J–L for control, Cotwin, and schizophrenia patients respectively. Overall, this analysis shows that the neurons derived from the affected twins had a very delayed maturation compared to the other 2 groups. At 2 months, when the neurons were more mature, most neurophysiological features split into 3 groups, where the neurons derived from the unaffected co-twins were in an intermediate state between the other two groups.

DISCUSSION

In this study, we differentiated DG granule hippocampal neurons from twin sets that were discordant for schizophrenia and compared them to control neurons that were derived from healthy twin sets. We found morphological, transcriptional, and neurophysiological changes in the patients' neurons compared to their co-twins and compared to the controls. This unique cohort of monozygotic twins that are discordant to schizophrenia allowed us to measure schizophrenia-related changes in a similar genetic background, reducing the heterogeneity that we usually need to address. The results point to synaptic deficits as a central phenotype of schizophrenia DG granule neurons. These deficits appear when the cells are approximately 8 weeks after the start of the differentiation which means that these are still pre-natal neurons and this means that the patients are biologically pre-deposed to the disease. When considering environment vs. genetic origins of the disease, our results emphasize that there is a genetic origin to the disease that may be aggravated by environmental stresses.

The neurons that were derived from the schizophrenia patients were smaller (less arborized with decreased capacitance), hypoexcitable (measured in patch-clamp as fewer evoked action
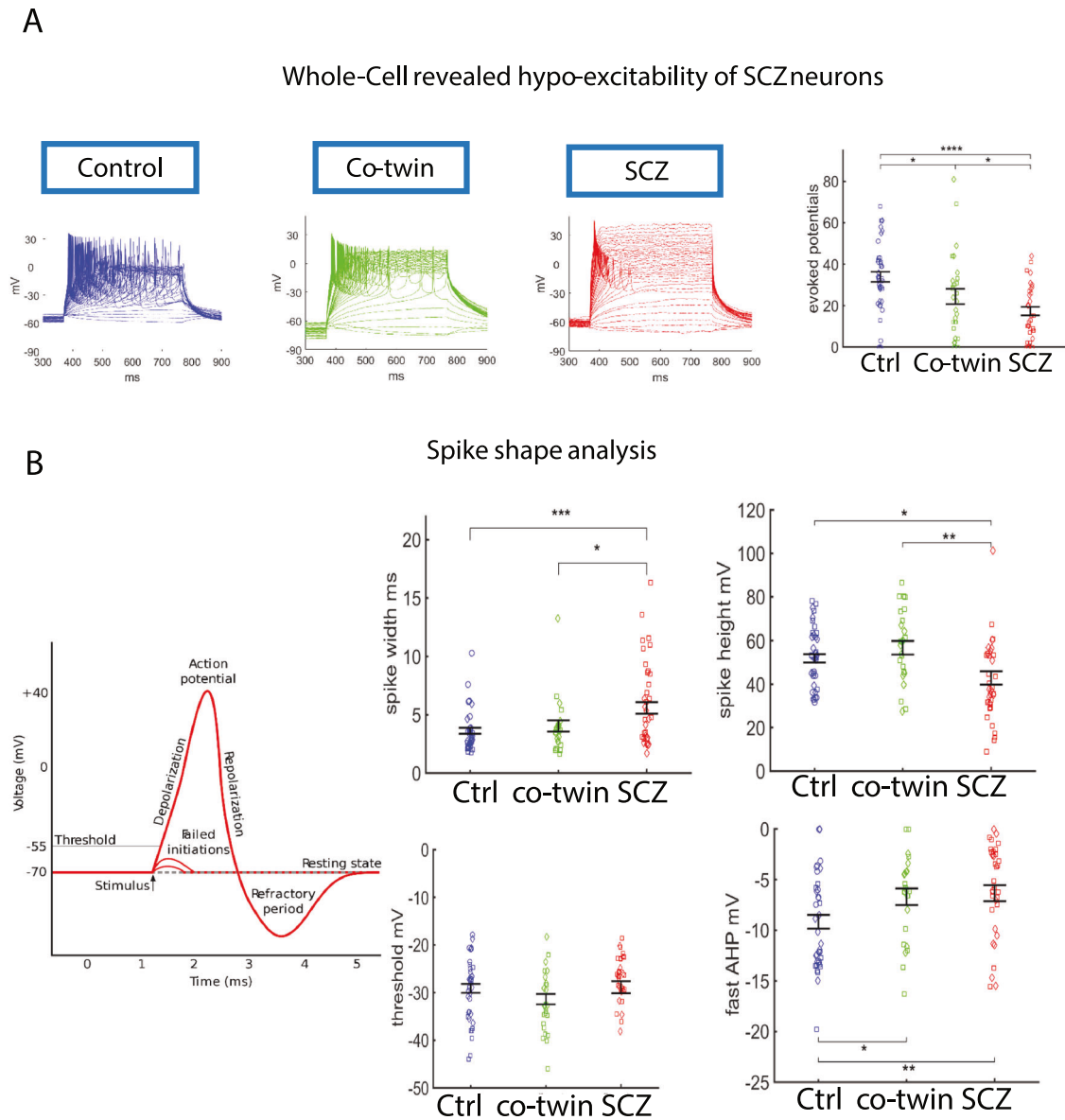
Fig. 5 Hypoexcitability of neurons derived from schizophrenia patients. A The neurons derived from the schizophrenia patients produced fewer evoked action potentials than the neurons derived from the other 2 groups. The neurons derived from the unaffected twin siblings (depressive disorder) produced more evoked action potentials than those from the affected twin siblings but fewer than the neurons derived from the healthy twin pairs. On the left are representative trace recordings. On the right, the averages of the total evoked potentials (see Methods) are presented. **B** Spike shape analysis. The spike width was wider in the neurons derived from the affected twin siblings compared to the other 2 groups. The spike amplitude was smaller in the neurons derived from the affected twin siblings compared to the neurons derived from the other 2 groups. There was no significant change in the threshold for eliciting an action potential between the 3 groups. The amplitude of the fast afterhyperpolarization (AHP) was smaller in the neurons derived from both the affected twin siblings and the unaffected twin siblings. The data acquired in this figure was obtained from 3-4 differentiation cycles for each of the lines. * represents $p < 0.05$, ** represents $p < 0.01$, *** represents $p < 0.001$, **** represents $p < 0.0001$.

potentials and on MEAs as reduced spontaneous activity and reduced number of bursts), with immature features of the action potential. They had reduced sodium and potassium currents and a decrease in their synaptic activity. The decrease in the synaptic activity may be caused and related to the delayed maturation of the schizophrenia neurons. The reduction that we observed in the EPSC rate in the affected siblings likely relates to presynaptic mechanisms. Yet, when analyzing the transcriptional changes, we see enrichment of genes of the "Postsynaptic cell membrane" pathway. This means that probably several synaptic mechanisms are deficient.

It is notable that one of the dysregulated pathways in the siblings with schizophrenia is Reg. of actin cytoskeleton, and this may be correlated with the reduced cell and dendritic tree size (Supplementary Fig. 2). Another dysregulated pathway is the "dentate gyrus development (Supplementary File 4) that may also be correlated with the less mature morphology in the schizophrenia neurons. The schizophrenia neurons had a more depolarized resting membrane potential and lower membrane resistance. It is interesting to note that both the affected twins had an overexpression of the KCNJ16 (Potassium Inwardly Rectifying Channel Subfamily J Member 16) gene. This overexpression may cause this increase in the input conductance of the neurons [53].

The neurons derived from the twin siblings that were unaffected by schizophrenia (depressive disorder) were in an intermediate state between their affected siblings and the healthy

SCZ neurons showed reduced Na⁺ and K+ currents upon voltage injection
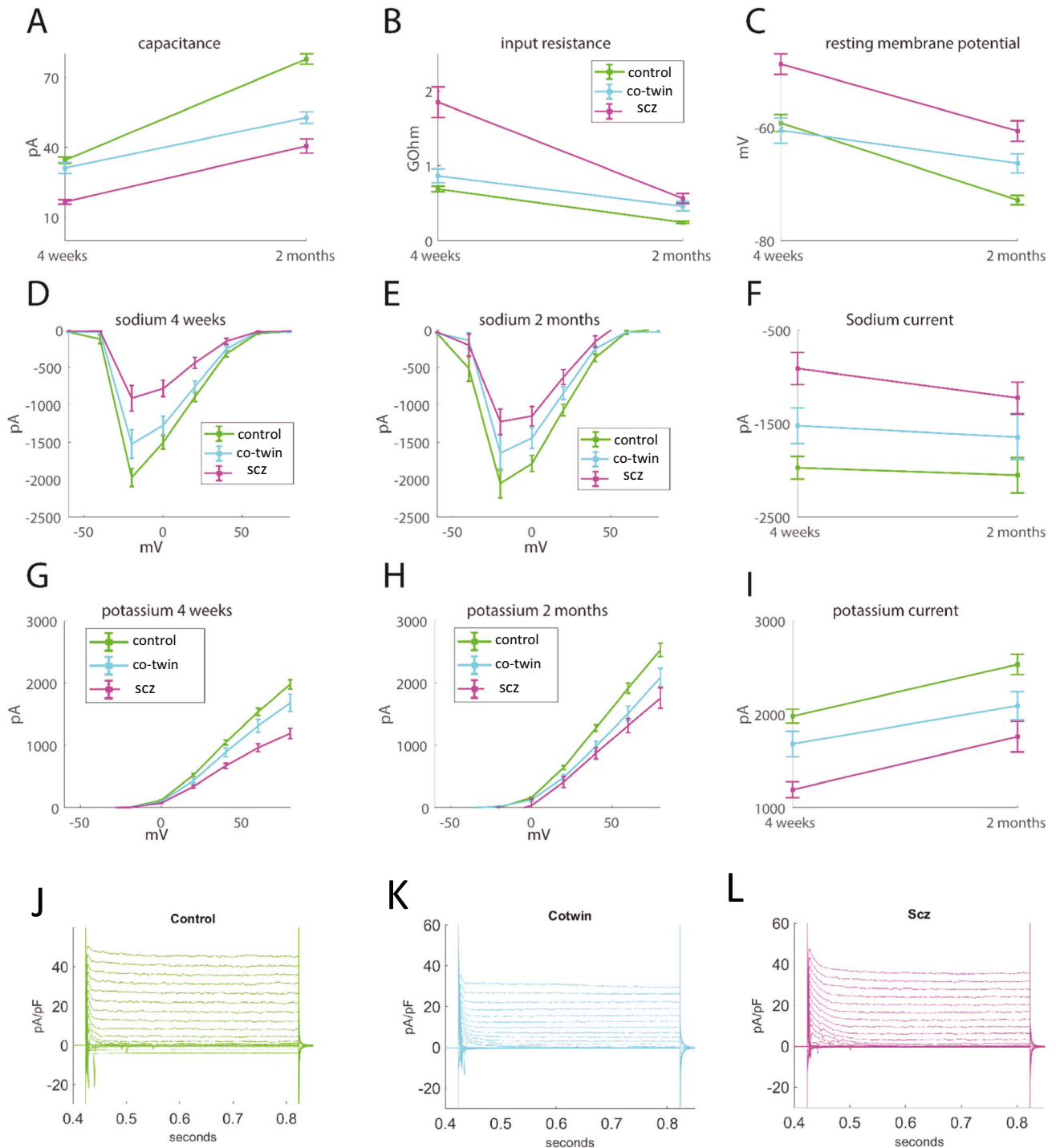

Fig. 6 Three groups were observed when analyzing neurophysiological features throughout the maturation of the DG granule neurons.
A The capacitance measurements of the 3 groups (neurons derived from the affected twin siblings, neurons derived from the unaffected co-twin siblings (depressive disorder), and neurons derived from the healthy twins) at 4 weeks and 2 months. **B** The input conductance measurements of the 3 groups at 4 weeks and 2 months. **C** The resting membrane potential of the 3 groups at 4 weeks and 2 months. **D** The sodium currents of the 3 groups at 4 weeks. **E** The sodium currents of the 3 groups at 2 months. **F** The sodium currents at -20 mV of the 3 groups at 4 weeks and 2 months. **G** The potassium currents of the 3 groups at 4 weeks. **H** The potassium currents of the 3 groups at 2 months. **I** The potassium currents at 20 mV of the 3 groups at 4 weeks and 2 months. **J** A representative example trace of the sodium and potassium currents acquired in voltage clamp mode of a control neuron. **K** A representative example trace of the sodium and potassium currents acquired in voltage clamp mode of a co-twin neuron. **L** A representative example trace of the sodium and potassium currents acquired in voltage clamp mode of a schizophrenia neuron. The data acquired in this figure was obtained from 3-4 differentiation cycles for each of the lines.

controls in many of the neurophysiology aspects that we measured. For example, the neurons from the unaffected siblings (depressive disorder) were also less arborized with reduced capacitance when compared to the control neurons but more arborized and with a higher capacitance when compared to the neurons derived from their siblings who were suffering from schizophrenia. Their membrane resistance was smaller than their affected twin but larger than the control twins. Similarly, their resting membrane potential was in between the schizophrenia patients and the controls. Their excitability when measured by the total number of action potentials was reduced compared to the control neurons but higher than the neurons derived from their affected twin siblings. However, when measuring the spontaneous activity by MEAs, they were more excitable than the controls (and both were more excitable than the affected twins). Their sodium currents were also larger than their affected twin sibling but smaller than the currents of the control neurons. Their synaptic currents were unaffected compared to the control neurons.

The synaptic connectivity was measured by the rate of EPSCs and was severely reduced in the affected twins compared to the other 2 groups. When calculating the 20 most differentially expressed genes between the twin sets with schizophrenia compared to the control twin sets, 6 were synapse-related. One of the dysregulated pathways in this comparison was the "anterograde trans-synaptic signaling." Furthermore, we compared the affected twins to the unaffected twins (depressive disorder), each twin set separately. For pair number 1, the 3 most dysregulated pathways were "Synapse," "Cell junction," and "Postsynaptic cell membrane." In pair 3, the most dysregulated functional annotations were similarly "Cell junction," "Postsynaptic cell membrane," and "Synapse." Clearly, a synaptic impairment was a strong phenotype of both the schizophrenia patients compared to their twin siblings both when measuring the synaptic signaling with patch-clamp and at the gene expression level. Synaptic impairments have been linked with schizophrenia in animal studies [54], in post mortem tissue [55, 56], and in patient-derived neurons [57]. Here we confirm that there is also a synaptic impairment in our DG granule patient-derived neurons. Our results are probably the strongest indication that a synaptic deficit is indeed a prominent phenotype of neurons derived from schizophrenia patients, as it is observed in the affected twins when measured in electrophysiology and not in the unaffected siblings (depressive disorder). However, at the gene expression level, there is a synaptic dysregulation also in the co-twins, but it is less profound.

The neurons derived from the schizophrenia patients also exhibited a decreased number of evoked action potentials, and the unaffected sibling (depressive disorder) was in an intermediate state between the affected twin and the healthy controls. A decreased number of evoked action potentials has also been previously reported in schizophrenia patients [34]. Interestingly, schizophrenia shares multiple genomic associations with bipolar disorder [58–60], but DG granule neurons derived from bipolar disorder patients are hyperexcitable whereas those derived from schizophrenia patients are hypoexcitable [29, 61, 62]. Our study shows that the unaffected twin (depressive disorder) also had fewer evoked potentials with current injections but, on the other hand, it had more spontaneous activity when measured with MEAs. This increased spontaneous activity may help to rescue these individuals as it strengthens network activity in a network where the synapses are deficient.

The RNA sequencing results indicate that the DG development pathway is dysregulated when comparing the control twins and the affected twins (both affected and unaffected twin siblings). Indeed, we see that the cells of the affected twins were smaller, with a reduced capacitance. The smaller membrane resistance observed in the affected twins also signifies that there is a delay in the expression of ion channels such as the inward rectifying

potassium channels and this is further supported by the more depolarized resting membrane potential. A delay in the development of gray and white matter in adolescent patients with schizophrenia has also been previously reported [63, 64]. Common genetic variants that affect rates of brain growth or atrophy, including the hippocampus, showed genetic overlap with schizophrenia in a recent meta-analysis of changes in brain morphology across the lifespan [65]. The DG newly born granule neurons are thought to be extremely important to the DG circuitry [66, 67]. Newly born DG granule neurons are formed throughout our lives, so this immature phenotype affects both the development and the integration of these delayed developing DG neurons continuously throughout the patients' lives.

Our study demonstrates several phenotypes of DG granule neurons derived from schizophrenia patients and their unaffected twin siblings (depressive disorder) that demonstrate only a partial list of these phenotypes. The synaptic impairment is a noticeable phenotype that appears both in the electrophysiological recordings and in the transcriptional analysis. This phenotype is much less prominent in the unaffected twin (depressive disorder), which further indicates the importance of hippocampal synaptic impairment in the mechanism of this disease. The DG is not the only affected area and synaptic deficits were also shown in patient-derived cortical neurons [68]. Here, we have focused on the DG and also had the advantage of this special cohort with a similar genetic background between the twins.

That both the unaffected and affected twin pair are morphologically and electro-physiologically different from control twins suggests an underlying germline genetic defect that is further supported by transcriptional profile differences. Epigenetic modifications can also be responsible for the disease onset in one of the patients. Since iPSC derived neurons are considered rejuvenated and the reprogramming process erases epigenetic and environmental changes, our study shows specifically the changes in the patients' neurons that are predisposed since birth. The ability to detect a phenotype using iPSC-derived neurons implies that genetic differences between the patients play an important role in schizophrenia. This means that the phenotypical changes that we measured in the derived neurons, may show relevant mechanisms for the symptoms in the individuals. It is important to mention, that the unaffected co-twins were later diagnosed with a depressive disorder. Previous postmortem studies have also observed that changes in the morphological features of subiculum neurons were also similar yet more pronounced in schizophrenia patients compared to patients with mood disorders [69]. Another study, measured the Layer III pyramidal cells in the prefrontal cortex using postmortem tissue similarly revealed changes in the morphology of patients with major depression, and the changes were more exacerbated in neurons from schizophrenia patients [70]. This strengthens our results that neurons derived from patients with mood disorders (the co-twins) exhibit morphological and synaptic alterations that are stronger in patients with schizophrenia (the affected twins). Furthermore, that we find morphological and electro-physiological differences between discordant twin pairs, that are further confirmed by transcriptional differences suggests that in addition to the proposed germline changes between schizophrenia and neurotypical controls there are likely somatic changes in the genomes of the affected or unaffected pair that occurred after the twins split following fertilization.

DATA AVAILABILITY

REFERENCES

1. Bhugra D. The global prevalence of schizophrenia. PLoS Med. 2005;2:e151.
2. Haro JM, Novick D, Bertsch J, Karagianis J, Dossenbach M, Jones PB. Cross-national clinical and functional remission rates: Worldwide Schizophrenia Out-patient Health Outcomes (W-SOHO) study. Br J Psychiatry. 2011;199:194–201.
3. Saha S, Chant D, Welham J, McGrath J. A systematic review of the prevalence of schizophrenia. PLoS Med. 2005;2:e141.
4. Wright IC, Rabe-Hesketh S, Woodruff PW, David AS, Murray RM, Bullmore ET. Meta-analysis of regional brain volumes in schizophrenia. Am J Psychiatry. 2000;157:16–25.
5. Tamminga CA, Stan AD, Wagner AD. The hippocampal formation in schizophrenia. Am J Psychiatry. 2010;167:1178–93.
6. Ellison-Wright I, Bullmore E. Meta-analysis of diffusion tensor imaging studies in schizophrenia. Schizophr Res. 2009;108:3–10.
7. Coyle JT. The glutamatergic dysfunction hypothesis for schizophrenia. Harv Rev Psychiatry. 1996;3:241–53.
8. Cioffi CL. Modulation of NMDA receptor function as a treatment for schizophrenia. Bioorg Med Chem Lett. 2013;23:5034–44.
9. Brisch R, Saniotis A, Wolf R, Bielau H, Bernstein HG, Steiner J, et al. The role of dopamine in schizophrenia from a neurobiological and evolutionary perspective: old fashioned, but still in vogue. Front Psychiatry. 2014;5:47.
10. Balu DT. The NMDA receptor and schizophrenia: from pathophysiology to treatment. Adv Pharmacol. 2016;76:351–82.
11. Vilain J, Galliot AM, Durand-Roger J, Leboyer M, Llorca PM, Schurhoff F, et al. [Environmental risk factors for schizophrenia: a review]. Encephale. 2013;39:19–28.
12. Narayan CL, Shikha D, Shekhar S. Schizophrenia in identical twins. Indian J Psychiatry. 2015;57:323–4.
13. Hilker R, Helenius D, Fagerlund B, Skytthe A, Christensen K, Werge TM, et al. Heritability of schizophrenia and schizophrenia spectrum based on the nationwide Danish twin register. Biol Psychiatry. 2018;83:492–8.
14. Cardno AG, Gottesman II. Twin studies of schizophrenia: from bow-and-arrow concordances to Star Wars Mx and functional genomics. Am J Med Genet. 2000;97:12–7.
15. Dennison CA, Legge SE, Pardinas AF, Walters JTR. Genome-wide association studies in schizophrenia: Recent advances, challenges and future perspective. Schizophr Res. 2020;217:4–12.
16. Ripke S, O'Dushlaine C, Chambert K, Moran JL, Kahler AK, Akterin S, et al. Genome-wide association analysis identifies 13 new risk loci for schizophrenia. Nat Genet. 2013;45:1150–9.
17. Schizophrenia Working Group of the Psychiatric Genomics C. Biological insights from 108 schizophrenia-associated genetic loci. Nature. 2014;511:421–7.
18. Schmidt-Kastner R, Guloksuz S, Kietzmann T, van Os J, Rutten BPF. Analysis of GWAS-derived schizophrenia genes for links to ischemia-hypoxia response of the brain. Front Psychiatry. 2020;11:393.
19. Choudhary A, Peles D, Nayak R, Mizrahi L, Stern S. Current progress in understanding schizophrenia using genomics and pluripotent stem cells: a meta-analytical overview. Schizophr Res. 2022.
20. Romanovsky E, Choudhary A, Abu Akel A, Stern S. Seeking convergence and divergence between autism and schizophrenia using genomic tools and patients' neurons. Preprint at https://doi.org/10.1101/2023.08.11.552921.
21. Lam M, Chen CY, Li Z, Martin AR, Bryois J, Ma X, et al. Comparative genetic architectures of schizophrenia in East Asian and European populations. Nat Genet. 2019;51:1670–8.
22. Huo Y, Li S, Liu J, Li X, Luo XJ. Functional genomics reveal gene regulatory mechanisms underlying schizophrenia risk. Nat Commun. 2019;10:670.
23. Thyme SB, Pieper LM, Li EH, Pandey S, Wang Y, Morris NS, et al. Phenotypic landscape of schizophrenia-associated genes defines candidates and their shared functions. Cell. 2019;177:478–91. e20.
24. Rajarajan P, Borrman T, Liao W, Schrode N, Flaherty E, Casino C, et al. Neuron-specific signatures in the chromosomal connectome associated with schizophrenia risk. Science. 2018;362:eaat4311.
25. He D, Fan C, Qi M, Yang Y, Cooper DN, Zhao H. Prioritization of schizophrenia risk genes from GWAS results by integrating multi-omics data. Transl Psychiatry. 2021;11:175.
26. Trubetskoy V, Pardinas AF, Qi T, Panagiotaropoulou G, Awasthi S, Bigdeli TB, et al. Mapping genomic loci implicates genes and synaptic biology in schizophrenia. Nature. 2022;604:502–8.
27. Takahashi K, Tanabe K, Ohnuki M, Narita M, Ichisaka T, Tomoda K, et al. Induction of pluripotent stem cells from adult human fibroblasts by defined factors. Cell. 2007;131:861–72.
28. Brennand KJ, Simone A, Jou J, Gelboin-Burkhart C, Tran N, Sangar S, et al. Modelling schizophrenia using human induced pluripotent stem cells. Nature. 2011;473:221–5.
29. Stern S, Santos R, Marchetto MC, Mendes APD, Rouleau GA, Biesmans S, et al. Neurons derived from patients with bipolar disorder divide into intrinsically different sub-populations of neurons, predicting the patients' responsiveness to lithium. Mol Psychiatry. 2018;23:1453–65.
30. Vadodaria KC, Ji Y, Skime M, Paquola A, Nelson T, Hall-Flavin D, et al. Serotonin-induced hyperactivity in SSRI-resistant major depressive disorder patient-derived neurons. Mol Psychiatry. 2019;24:795–807.
31. Mertens J, Herdy JR, Traxler L, Schafer ST, Schlachetzki JCM, Bohnke L, et al. Age-dependent instability of mature neuronal fate in induced neurons from Alzheimer's patients. Cell Stem Cell. 2021;28:1533–48. e6.
32. Hussein Y, Tripathi U, Choudhary A, Nayak R, Peles D, Rosh I, et al. Early maturation and hyperexcitability is a shared phenotype of cortical neurons derived from different ASD-associated mutations. Transl Psychiatry. 2023;13:246.
33. Stern S, Lau S, Manole A, Rosh I, Percia MM, Ben Ezer R, et al. Reduced synaptic activity and dysregulated extracellular matrix pathways in midbrain neurons from Parkinson's disease patients. NPJ Parkinson's disease. 2022;8:103.
34. Sarkar A, Mei A, Paquola ACM, Stern S, Bardy C, Klug JR, et al. Efficient generation of CA3 neurons from human pluripotent stem cells enables modeling of hippocampal connectivity in vitro. Cell Stem Cell. 2018;22:684–97. e9.
35. Chiang CH, Su Y, Wen Z, Yoritomo N, Ross CA, Margolis RL, et al. Integration-free induced pluripotent stem cells derived from schizophrenia patients with a DISC1 mutation. Mol Psychiatry. 2011;16:358–60.
36. Pedrosa E, Sandler V, Shah A, Carroll R, Chang C, Rockowitz S, et al. Development of patient-specific neurons in schizophrenia using induced pluripotent stem cells. J Neurogenet. 2011;25:88–103.
37. Uzuneser TC, Speidel J, Kogias G, Wang AL, de Souza Silva MA, Huston JP, et al. Disrupted-in-schizophrenia 1 (DISC1) overexpression and juvenile immune activation cause sex-specific schizophrenia-related psychopathology in rats. Front Psychiatry. 2019;10:222.
38. Page SC, Sripathy SR, Farinelli F, Ye Z, Wang Y, Hiler DJ, et al. Electrophysiological measures from human iPSC-derived neurons are associated with schizophrenia clinical status and predict individual cognitive performance. Proc Natl Acad Sci USA. 2022;119:e2109395119.
39. Tavitian A, Song W, Schipper HM. Dentate gyrus immaturity in schizophrenia. Neuroscientist. 2019;25:528–47.
40. Bohlken MM, Brouwer RM, Mandl RC, Van den Heuvel MP, Hedman AM, De Hert M, et al. Structural brain connectivity as a genetic marker for schizophrenia. JAMA Psychiatry. 2016;73:11–9.
41. Brant B, Stern T, Shekhidem HA, Mizrahi L, Rosh I, Stern Y, et al. IQSEC2 mutation associated with epilepsy, intellectual disability, and autism results in hyper-excitability of patient-derived neurons and deficient synaptic transmission. Mol Psychiatry. 2021;26:7498–508.
42. Yuan SH, Martin J, Elia J, Flippin J, Paramban RI, Hefferan MP, et al. Cell-surface marker signatures for the isolation of neural stem cells, glia and neurons derived from human pluripotent stem cells. PLoS ONE. 2011;6:e17540.
43. Dobin A, Davis CA, Schlesinger F, Drenkow J, Zaleski C, Jha S, et al. STAR: ultrafast universal RNA-seq aligner. Bioinformatics. 2013;29:15–21.
44. Love MI, Huber W, Anders S. Moderated estimation of fold change and dispersion for RNA-seq data with DESeq2. Genome Biol. 2014;15:550.
45. Jaffe AE, Hoeppner DJ, Saito T, Blanpain L, Ukaigwe J, Burke EE, et al. Profiling gene expression in the human dentate gyrus granule cell layer reveals insights into schizophrenia and its genetic risk. Nat Neurosci. 2020;23:510–9.
46. Santos R, Linker SB, Stern S, Mendes APD, Shokhirev MN, Erikson G, et al. Deficient LEF1 expression is associated with lithium resistance and hyperexcitability in neurons derived from bipolar disorder patients. Mol Psychiatry. 2021;26:2440–56.
47. Hoseth EZ, Krull F, Dieset I, Morch RH, Hope S, Gardsjord ES, et al. Exploring the Wnt signaling pathway in schizophrenia and bipolar disorder. Transl Psychiatry. 2018;8:55.
48. Okerlund ND, Cheyette BN. Synaptic Wnt signaling-a contributor to major psychiatric disorders? J Neurodev Disord. 2011;3:162–74.
49. Hussaini SM, Choi CI, Cho CH, Kim HJ, Jun H, Jang MH. Wnt signaling in neuropsychiatric disorders: ties with adult hippocampal neurogenesis and behavior. Neurosci Biobehav Rev. 2014;47:369–83.
50. Wei Z, Wang L, Xuan J, Che R, Du J, Qin S, et al. Association analysis of serotonin receptor 7 gene (HTR7) and risperidone response in Chinese schizophrenia patients. Prog Neuropsychopharmacol Biol Psychiatry. 2009;33:547–51.
51. Ikeda M, Iwata N, Kitajima T, Suzuki T, Yamanouchi Y, Kinoshita Y, et al. Positive association of the serotonin 5-HT7 receptor gene with schizophrenia in a Japanese population. Neuropsychopharmacology. 2006;31:866–71.
52. Han EB, Stevens CF. Development regulates a switch between post- and pre-synaptic strengthening in response to activity deprivation. Proc Natl Acad Sci USA. 2009;106:10817–22.
53. Stern S, Segal M, Moses E. Involvement of potassium and cation channels in hippocampal abnormalities of embryonic Ts65Dn and Tc1 trisomic mice. EBioMedicine. 2015;2:1048–62.

54. Obi-Nagata K, Temma Y, Hayashi-Takagi A. Synaptic functions and their disruption in schizophrenia: From clinical evidence to synaptic optogenetics in an animal model. Proc Jpn Acad Ser B Phys Biol Sci. 2019;95:179–97.

55. Berdenis van Berlekom A, Muflihah CH, Snijders G, MacGillavry HD, Middeldorp J, Hol EM, et al. Synapse pathology in schizophrenia: a meta-analysis of postsynaptic elements in postmortem brain studies. Schizophr Bull. 2020;46:374–86.

56. Osimo EF, Beck K, Reis Marques T, Howes OD. Synaptic loss in schizophrenia: a meta-analysis and systematic review of synaptic protein and mRNA measures. Mol Psychiatry. 2019;24:549–61.

57. Sellgren CM, Gracias J, Watmuff B, Biag JD, Thanos JM, Whittredge PB, et al. Increased synapse elimination by microglia in schizophrenia patient-derived models of synaptic pruning. Nat Neurosci. 2019;22:374–85.

58. Bipolar D, Schizophrenia Working Group of the Psychiatric Genomics Consortium. Electronic address drve, Bipolar D, Schizophrenia Working Group of the Psychiatric Genomics C. Genomic dissection of bipolar disorder and schizophrenia, including 28 subphenotypes. Cell. 2018;173:1705–15. e16.

59. Bigdeli TB, Fanous AH, Li Y, Rajeevan N, Sayward F, Genovese G, et al. Genome-wide association studies of schizophrenia and bipolar disorder in a diverse cohort of US veterans. Schizophr Bull. 2021;47:517–29.

60. Lichtenstein P, Yip BH, Bjork C, Pawitan Y, Cannon TD, Sullivan PF, et al. Common genetic determinants of schizophrenia and bipolar disorder in Swedish families: a population-based study. Lancet. 2009;373:234–9.

61. Stern S, Sarkar A, Galor D, Stern T, Mei A, Stern Y, et al. A physiological instability displayed in hippocampal neurons derived from lithium-nonresponsive bipolar disorder patients. Biol Psychiatry. 2020;88:150–8.

62. Stern S, Sarkar A, Stern T, Mei A, Mendes APD, Stern Y, et al. Mechanisms underlying the hyperexcitability of CA3 and dentate gyrus hippocampal neurons derived from patients with bipolar disorder. Biol Psychiatry. 2020;88:139–49.

63. Douaud G, Mackay C, Andersson J, James S, Quested D, Ray MK, et al. Schizophrenia delays and alters maturation of the brain in adolescence. Brain. 2009;132:2437–48.

64. Cannon M, Caspi A, Moffitt TE, Harrington H, Taylor A, Murray RM, et al. Evidence for early-childhood, pan- developmental impairment specific to schizophreniform disorder: results from a longitudinal birth cohort. Arch Gen Psychiatry. 2002;59:449–56.

65. Brouwer RM, Klein M, Grasby KL, Schnack HG, Jahanshad N, Teeuw J, et al. Genetic variants associated with longitudinal changes in brain structure across the lifespan. Nat Neurosci. 2022;25:421–32.

66. Vivar C, van Praag H. Functional circuits of new neurons in the dentate gyrus. Front Neural Circuits. 2013;7:15.

67. Tashiro A, Sandler VM, Toni N, Zhao C, Gage FH. NMDA-receptor-mediated, cell-specific integration of new neurons in adult dentate gyrus. Nature. 2006;442:929–33.

68. Rasanen N, Tiihonen J, Koskuvi M, Lehtonen S, Koistinaho J. The iPSC perspective on schizophrenia. Trends Neurosci. 2022;45:8–26.

69. Rosoklija G, Toomayan G, Ellis SP, Keilp J, Mann JJ, Latov N, et al. Structural abnormalities of subicular dendrites in subjects with schizophrenia and mood disorders: preliminary findings. Arch Gen Psychiatry. 2000;57:349–56.

70. Larsen NY, Vihrs N, Moller J, Sporring J, Tan X, Li X, et al. Layer III pyramidal cells in the prefrontal cortex reveal morphological changes in subjects with depression, schizophrenia, and suicide. Transl Psychiatry. 2022;12:363.

AUTHOR CONTRIBUTIONS
Shani Stern designed experiments, performed patch clamp experiments, performed analysis, and wrote the article, Lei Zhang designed experiments, performed patch clamp experiments, performed analysis, Meiyan Wang designed experiments, grew the neurons and performed RNA purification, and performed analysis, Rebecca Wright performed patch clamp experiments and analysis, Idan Rosh performed patch clamp experiments and analysis, Yara Hussein performed analysis of RNA sequencing results, Tchelet Stern performed analysis of RNA sequencing and patch clamp results, Ashwani Choudhary grew neurons and performed immunohistochemistry, imaging, and analysis, Utkarsh Tripathi performed analysis of immunohistochemistry images, Patrick Reed performed analysis of RNA sequencing results, Hagit Sadis performed analysis of RNA sequencing results, Ritu Nayak grew neurons and performed RNA extraction, Aviram Shemen performed patch clamp experiments, Karishma Agarwal performed immunohistochemistry, Diogo Cordeiro wrote the introduction of the article, David Peles performed analysis of GWAS and RNA sequencing unified genes results, Yuqing Hang performed analysis of RNA sequencing results, Ana P. D. Mendes grew neurons, Tithi D. Baul designed experiments and grew neurons, Julien G. Roth designed experiments and grew neurons, Shashank Coorapati performed analysis of morphological features of the neurons, Marco P. Boks designed experiments, W. Richard McCombie designed experiment, Hilleke Hulshoff Pol designed experiments, Kristen J. Brennand designed experiments and grew cells, János M Réthelyi designed experiments and grew cells, René S. Kahn designed experiments and diagnosed patients, Maria C. Marchetto designed experiments, grew cells, and performed RNA extractions, Fred H. Gage designed experiments and edited the manuscript.

COMPETING INTERESTS
The authors declare no competing interests.

ADDITIONAL INFORMATION
Supplementary information The online version contains supplementary material available at https://doi.org/10.1038/s41380-024-02561-1.

Correspondence and requests for materials should be addressed to Shani Stern or Fred H. Gage.

Reprints and permission information is available at http://www.nature.com/reprints

Publisher's note Springer Nature remains neutral with regard to jurisdictional claims in published maps and institutional affiliations.